

## DAMPED ACCELERATOR STRUCTURES\*

H. DERUYTER, Z. D. FARKAS, H. A. HOAG, K. KO, N. KROLL,<sup>†</sup> G. A. LOEW,  
R. H. MILLER, R. B. PALMER, J. M. PATERSON, J. W. WANG  
Stanford Linear Accelerator Center, Stanford University, Stanford, CA 94309, USA

## Introduction

This paper reports continuing work on high-gradient accelerator structures for future TeV linear colliders. A prerequisite of these structures is that they heavily damp wakefield modes which can be induced by  $e^\pm$  bunch trains. Disk-loaded waveguide structures under investigation have radial slots in the disks and/or radial rectangular waveguides in the cavity walls to couple wakefield power out to external lossy regions. We discuss a high-power S-Band experiment with a short standing-wave section to determine whether the peak field breakdown threshold is lowered by the presence of slots in the disks. Next, we describe low-power measurements on structure models at S-Band and X-Band to identify mode frequencies and  $Q$  values.

## Track 1 High-Power Test

Work at SLAC on damped accelerator structures was begun in 1988. An earlier paper<sup>1</sup> described preliminary low-power testing of the four-cavity S-Band standing-wave structure shown in fig. 1.

For the high-power test, the structure was installed in a test system<sup>2</sup> connected to a high-power klystron. After initial pumping and bakeout at 250°C, the structure was gradually

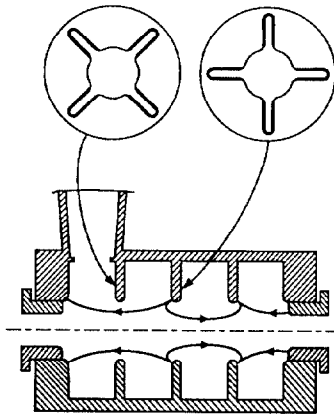


Figure 1: Cross-sections of Track 1 slotted disk structure.

Table 1: Breakdown-limited gradient for  $2\pi/3$  slotted-disk structure.

Frequency	MHz	2857
Iris diameter	cm	3.6
Total length	cm	21
Filling time*	$\mu$ s	0.87
Pulse length	$\mu$ s	1.5–2.5
Peak power input	MW	21.5
$E_s$	MV/m	315
$E_s/E_{acc}$ for SW structure		$5.10^\dagger$

\* Assuming critical coupling.

<sup>†</sup> The relative number obtained from MAFIA (4.86) was corrected to give 5.10 by normalizing it to SUPERFISH.

\* Work supported by Department of Energy contract DE-AC03-76SF00515.

<sup>†</sup> Permanent address: University of California, San Diego, La Jolla, CA 92093, USA.

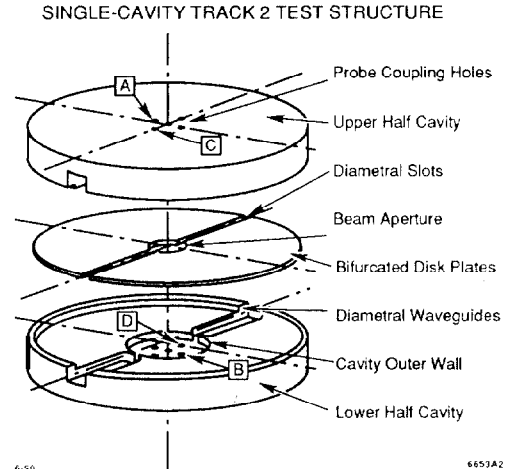


Figure 2: Single-cavity Track 2 with half-disks.

RF processed up to the maximum field level sustainable. Some initial processing was done in argon at a pressure between 1 and  $5 \times 10^{-6}$  Torr. This produced some reduction in the field enhancement factor, but most of the RF processing was done under high vacuum, with the structure steadily outgassing at pressures between  $10^{-8}$  and  $10^{-9}$  Torr. A spiral of increasing RF power from the klystron, breakdown, recovery and further increase was followed up to a level of 21.5 MW, at which breakdown persisted and could not be processed away. Table 1 summarizes the levels reached.

It was determined from MAFIA that the ratio of the surface field ( $E_s$ ) to the axial accelerating field ( $E_{acc}$ ) was increased 8% by the presence of the slots.

## Low-power tests with an S-Band slotted disk structure

The first structure investigated (Track 2) is best thought of as a conventional disk-loaded cylindrical waveguide in which the disks are divided into four quadrants by four orthogonal radial slots. The slotted disk quadrants continue radially outward past the walls of the cavities, transforming into double-ridged waveguides. These waveguides are dimensioned so their  $TE_{10}$  mode cutoff is below the frequencies of all resonances of the accelerator cavities. The fundamental accelerating mode of the structure is nevertheless undamped because its symmetry is such that it does not couple to the  $TE_{10}$  mode of the waveguide.

An exploded view of a single-cavity version of Track 2 with a double-slotted disk is shown in fig. 2. This simplified structure is able to support only the 0 and  $\pi$  modes, which facilitates understanding its behavior. Figures 3 through 5 show network analyzer  $S_{21}$  plots obtained with coaxial  $E$  probes inserted in the designated end-plate holes (fig. 2).

With probes in C and D, the 0 and  $\pi$  resonances for the first two branches of the dispersion curve are shown in fig. 3. The dipole mode fields are oriented so that they do not couple to the ridged waveguides. When probes are inserted in A and B, the fields for the dipole  $\pi$  mode couple to the waveguides which, when shorted at equal radial distances from the structure axis, form a coupled-cavity system with multiple resonances above and below the fixed dipole 0 mode resonance. As the waveguide lengths are decreased or increased, the resonances move up or down in frequency, respectively. A method for determining the external  $Q$  ( $Q_e$ ) and resonant frequency ( $f_r$ )

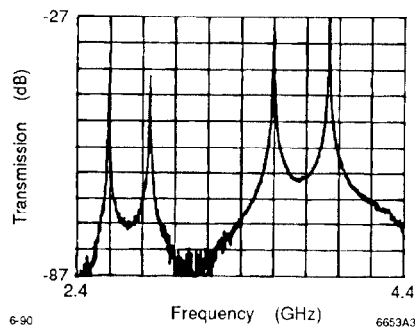


Figure 3: Single-cavity Track 2 resonances decoupled from waveguides.

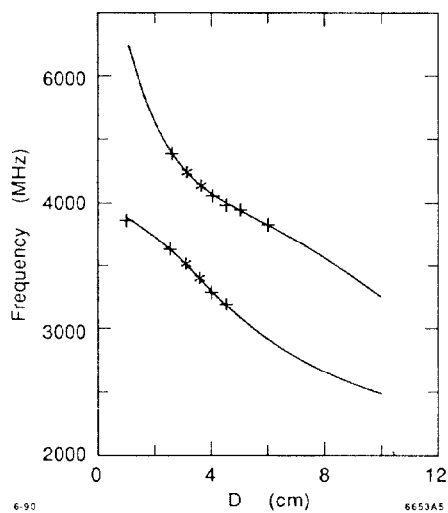


Figure 4: Measured single-cavity Track 2 waveguide resonance frequencies as a function of waveguide length, compared to the predictions of ref. 3.

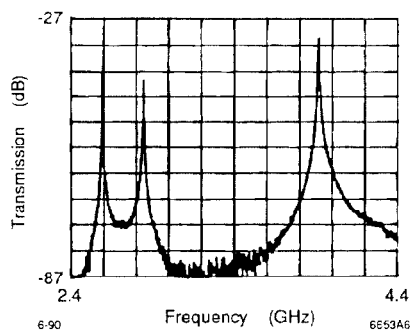


Figure 5: Single-cavity Track 2 resonances coupled to terminated waveguides.

of a cavity mode from the frequency dependence of coupled cavity/waveguide modes upon shorted waveguide length has been described.<sup>3</sup> The method gives a four-parameter formula for this dependence. Two of the parameters are  $Q_e$  and  $f_r$ . Figure 4 shows the results of applying this method to the dipole  $\pi$  mode. The four parameters are determined by fitting to the starred experimental points. This fit yields  $Q_e = 8.1 \pm 18\%$  and  $f_r = 3939 \pm 0.5\%$  MHz. The solid curves shown represent the prediction of the formula using the fitted parameters, and the points marked + are the remaining experimental measurements. Agreement between the data and the curves is satisfactory, but the precision of the fitted parameters is limited by the inexact measurement of waveguide length. When the wave-

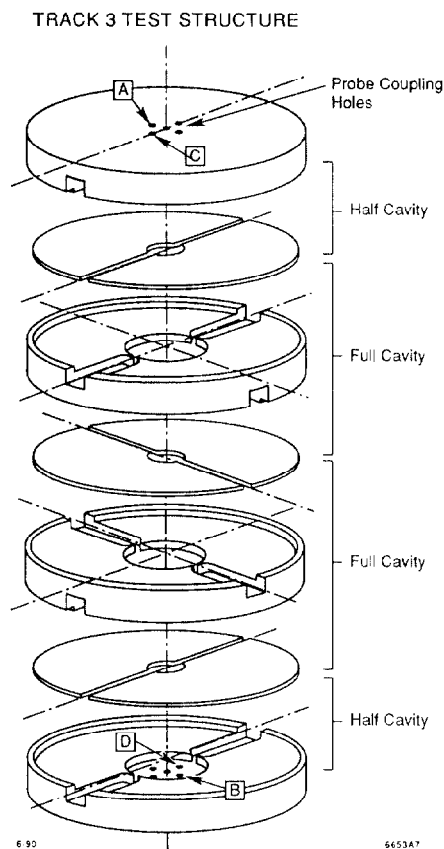


Figure 6: Track 3 experimental structure.

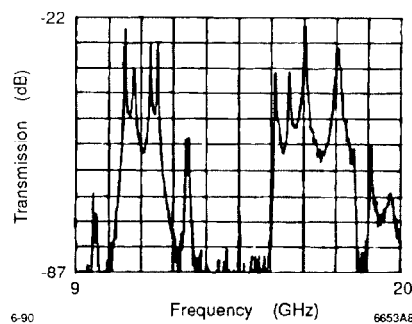


Figure 7: Track 3 resonances with A-B probe coupling.

guides are left open at their outer ends, some power radiates outward, lowering the resonance  $Q_s$ . When the waveguides are terminated, the  $Q_s$  become too low to measure (fig. 5). Thus it can be concluded that the Track 2 structure as described at the beginning of this section will effectively damp the dipole  $\pi$  mode when the radial ridged waveguides are well terminated.

#### Low-power tests on an X-Band slotted disk structure

Figure 6 illustrates our Track 3 experiment, which is an X-Band version of the slotted disk structure described above. Although the final structure is perceived as having four slots per disk, Track 3 retains the simplification of two slots per disk as an aid to interpreting the observed resonances.

Figure 7 shows the resonances on the fundamental ( $TM_{01}$ ) branch of the structure dispersion curve, and the dipole resonances on the second branch which would be excited by wake-fields. The ridged waveguides are shorted at their outer ends, and the probes are in the A and B positions. Since the test

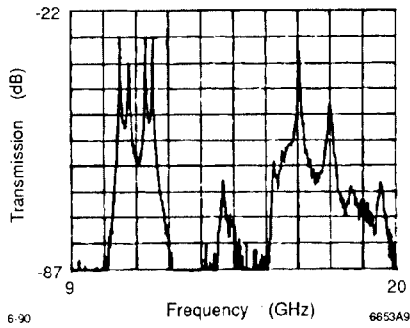


Figure 8: Track 3 with *A-B* probe coupling and waveguides terminated.

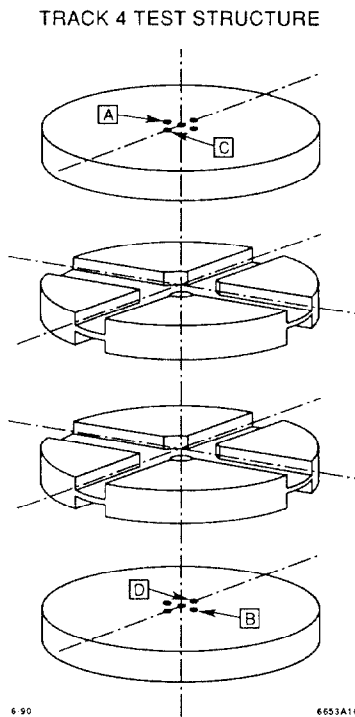


Figure 9: X-Band waveguide cross structure (Track 4).

structure is a three-cavity resonant stack, four resonances on each branch ( $0$ ,  $\pi/3$ ,  $2\pi/3$ , and  $\pi$ ) are observed. The fundamental accelerating mode does not couple because of symmetry. However, the dipole mode fields couple to the ridged waveguides (except for the  $0$  mode). As explained for Track 2, the shorted waveguides and the center cavities form a coupled resonator system, resulting in resonance doublets whenever the waveguides are multiples of a half-wavelength long. Well-matched terminations for the ridged waveguides were not available at the time of the test. The effect of inserting lossy plastic foam in the end of each guide is shown in fig. 8. Observe that most of the dipole modes are heavily damped. When the probes are in positions *C* and *D*, a different spectrum of dipole mode resonances is seen because the axial distributions of the standing-wave mode field patterns couple differently to the disk slots. It is concluded again that, with the full four-slot disk structure, all the most dangerous low-order dipole modes will be sufficiently damped.

#### Low-power tests on an X-Band crossed waveguide structure (Track 4)

The crossed waveguide arrangement (fig. 9) has the property of trapping the fundamental (accelerating) mode and coupling out the dipole and higher-order modes.

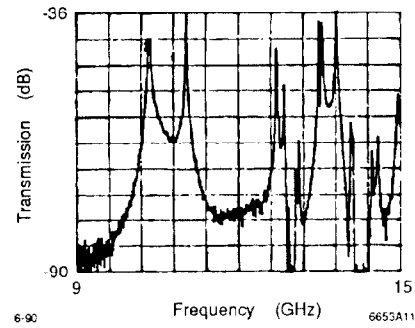


Figure 10: Track 4 single cavity resonances with waveguides shorted.

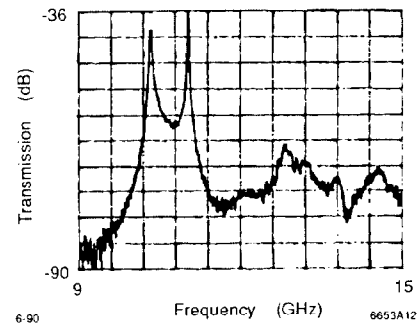


Figure 11: Track 4 single cavity resonances with waveguides terminated.

The geometry possibly has the advantage of being easier to fabricate. The waveguide width and the diameter of the small remaining segments of the central cylindrical cavity must be chosen carefully so that the waveguide  $TE_{10}$  mode cutoff lies above the frequency of the fundamental accelerating mode and below the frequency of the dipole  $\pi$  mode. Figure 10 shows the resonances obtained with a single cavity, with the outer ends of the rectangular waveguides shorted. The resonance patterns are independent of coupling probe positions in the end-plates because the crossed waveguides couple to all mode orientations. Again, a multiplicity of resonances above the fundamental  $0$  and  $\pi$  are observed because of coupling between the shorted waveguides and the central cavity. With longer guides, the number of resonances increases. When the guides are terminated, first-order dipole resonances above the fundamental pair are heavily damped, as shown in fig. 11.

#### Conclusion

Work on the structures described above has demonstrated that they can couple dipole mode power out of the central cavity region which supports the  $TM_{01}$  accelerating fields. The problem currently receiving attention is how to absorb this power in a very limited radial space, since magnetic focusing and other considerations make it very desirable to minimize the diameter of the complete structure.

#### References

- [1] "Damped Accelerator Structures for Future Linear  $e^\pm$  Colliders," H. Deruyter et al, *Proc. 1989 IEEE Part. Acc. Conf.*, p. 156.
- [2] "RF Breakdown Studies in Copper Electron Linac Structures," J. W. Wang and G. A. Loew, *Proc. 1989 IEEE Part. Acc. Conf.*, p. 1137.
- [3] "Computer Determination of the External Q and Resonant Frequency of Waveguide Loaded Cavities," N. M. Kroll and D. U. L. Yu, SLAC-PUB-5171, January 1990.